Pirti A and Eren M (2025)
Nova Geodesia 5(1):286
Research Article

Positional accuracy evaluation of CORS VRS, PPK, static GPS + GLONASS, and total station surveys in urban areas

Atinç PIRTI, Mehmet EREN

Yildiz Technical University, Department of Surveying Engineering, Davutpasa Campus, 34220 Esenler, Istanbul, Turkey; atinc@yildiz.edu.tr; meren@yildiz.edu.tr

Abstract

In urban environments, GNSS positioning is challenging due to signal blockage and multipath effects of surrounding buildings. This study evaluates the compatibility of CORS-VRS, PPK and static GNSS methods with total station measurements to investigate their accuracy in urban conditions. For this purpose, measurements were conducted in Esenler, Istanbul on 30 September 2020. Three measurement points (P1, P2 and P3) with varying levels of obstruction were selected. The results demonstrate that static GNSS measurements (with horizontal and vertical components below 5 mm and 11 mm, respectively) are the method with the highest positional accuracy. Conversely, PPK measurements exhibited larger deviations (0.857 m (X), 0.356 m (Y), and 0.780 m (Z) in P1, 0.302 m (X), 0.215 m (Y), and 0.255 m (Z) in P1, and 0.516 m (X), 0.284 m (Y), and 0.374 m (Z) in P3. Conversely, CORS-VRS measurements exhibited deviations ranging from 13 cm to 34 cm at baseline distances when compared to total station results. The findings demonstrate that while CORS-VRS and PPK can achieve sub-decimeter accuracy, they are significantly affected by multipath and signal blockages in dense urban environments. Thus, GNSS-based positioning in urban settings should be supplemented with total station surveys when high precision (1-2 cm) is required.

Keywords: CORS-VRS; GNSS accuracy; positioning precision; PPK; Static GNSS; Total station; Urban Multipath Effects

Introduction

Increasingly, the positions of utilities are being coordinated with high accuracy to update spatial databases. The features that are surveyed include manholes, covers, and hydrants, distribution boxes for water, gas, and electricity. The features are often in locations where buildings and tree cover prohibit the exclusive use of GNSS to coordinate such features. In urban environments, GNSS location accuracy is significantly compromised due to obstructions such as buildings, trees, and other structures (Feng *et al.,* 2020; Jones *et al.,* 2022; Hamza *et al.,* 2023; Wang, 2023). These obstacles can lead to signal degradation/complete blocking, especially when the number of visible satellites is less than four, which affects positioning accuracy (Yang *et al.*, 2017). Urban landscapes dominated by large surfaces such as walls and roofs complicate GNSS surveys because the signals reflected from these surfaces (multipath) affect the actual position of the receiver (James and

Received: 08 Jan 2025. Received in revised form: 11 Feb 2025. Accepted: 24 Feb 2025. Published online: 24 Feb 2025.

Quinton, 2013). This phenomenon is further aggravated when GNSS receivers are positioned close to the ground where the signal is completely blocked (Zhou *et al.*, 2004; Zhang *et al.* 2021; Hamza *et al.*, 2023; Viler *et al.*, 2023).

To reduce these difficulties, total stations are often used to survey infrastructure facilities (e.g., manholes, fire hydrants, etc.). However, the effectiveness of total stations can be hindered by urban traffic and parked vehicles, which may require crossing to establish checkpoints (Chen *et al.*, 2019). This process can be time-consuming as it requires careful exploration of the area to determine suitable routes for crossing (Mai et al., 2022). After crossing, total stations can effectively use features such as precise location determination, but such difficulties at the beginning of urban survey are a significant obstacle (Erenoglu *et al.*, 2018; Smith *et al.*, 2021; Hamza *et al.*, 2023, Viler *et al.*, 2023).

In urban areas, specific problems occur with the reception of signals because of the buildings. The accuracy with which a position can be determined is largely dependent on the type of measurement. For static surveys, a receiver is set up at a specific point. GNSS surveys can be categorized into static and kinematic methods, each with different advantages and limitations. Positions are determined over a relatively long period of time and are derived from the averages of these measurements after extreme values have been filtered out. This is mainly due to the considerable change in satellite geometry over the long observation time span (Xie and Petovello, 2014; Suzuki and Kubo, 2015; Wang *et al.*, 2019; Hayamizu and Nakata, 2023; Zhang *et al.* 2021; Viler *et al.*, 2023). İn contrast, kinematic GNSS measurement, positions are determined continuously for a series of points along a line. For each point, the position is determined only once. The distance between two surveys is dependent on the time interval between two position calculations by the receiver and on the speed at which the receiver and the antenna are being moved. For kinematic GNSS surveys, no stable mean average can be gained; each measured position is an independent value. Because the antenna is moved, environmental conditions for signal reception constantly change. Kinematic GNSS surveys must therefore be classified as providing relatively poor end results (Sideris, 2014; Zhang *et al.* 2021; Hamza *et al.*, 2023; Viler *et al.*, 2023; Li *et al.*, 2020; Li *et al.*, 2021). This is why the quality of kinematic survey is much more dependent on a good constellation of satellites than is the case with static survey.

GNSS network architectures often make use of multiple reference stations. This approach allows a more precise modelling of distance-dependent systematic errors principally caused by ionospheric and tropospheric refractions and satellite orbit errors (Gallo *et al.*, 2002). More specifically, a GNSS network decreases the dependence of the error budget on the distance of the nearest antenna. The network of receivers is linked to a computation center, and each station contributes its raw data to help create network-wide models of the distance-dependent errors. The computation of errors based on the full network's carrier phase measurements involves, first of all, the resolution of carrier phase ambiguities and requires knowledge of the reference station positions. At the same time the rover calculates its approximate position and transmits this information to the computation server, for example, via GSM or GPRS using a standard National Marine Electronics Association (NMEA) format. The computation center generates in real time a virtual reference station (VRS) at or near the initial rover position. This is done by geometrically translating the pseudorange and carrier phase data from the closest reference station to the virtual location and then adding the interpolated errors from the network error models. The idea of the VRS, or virtual base station (VBS), introduced by Trimble is that a base station is artificially created in the vicinity of a rover receiver. All baseline-length-dependent errors, such as abnormal troposphere variation, ionospheric disturbances, and orbital errors, are reduced for this VRS (França *et al.*, 2021, Ghilani and Wolf, 2012). The rover receiving VRS information has a lower level of these errors than a distant base station (Wang and Yan, 2015). The VRS is computed for a position supplied by the rover during communication start-up with networking software. The VRS position can change if the rover is far away from the initial point. The format for sending the rover's position is standard NMEA format. Most rovers receive VRS data for a calculated base station that is within a couple of meters away. The VRS approach requires bi-directional communication for supplying the rover's position to the networking software (El-Mowafy, 2000;

Pirti *et al.*, 2013; Suzuki and Kubo, 2015; Pirti, 2016; Wolf *et al.*, 2018; Zhang *et al.*, 2021; Hamza *et al.*, 2023; Viler *et al.*, 2023; Ning et al., 2018).

The integration of GNSS with Inertial Navigation Systems (INS) improves urban positioning. The hybrid approach, where these two systems are used together, compensates for the time period when GNSS signals are absent or weak, such as in urban areas where signals are blocked (Ning *et al.*, 2018; Feng *et al.*, 2020). Recent studies have shown that integrated GNSS/INS systems significantly increase navigation position accuracy by supporting continuous position updates even in difficult conditions (Li *et al.*, 2021; Zhang *et al.*, 2021; Hamza *et al.*, 2023; Viler *et al.*, 2023; Wang, 2023).

This paper presents a general comparative assessment of different GNSS measurement methods, namely CORS-VRS, PPK and static GNSS, on total station data in urban environments. The study systematically investigates the impact of urban obstacles, multiple paths and signal blockages on GNSS positioning accuracy by selecting three representative measurement points, namely P1, P2 and P3, representing highly obstructed, moderately obstructed and clear sky conditions, respectively. It also aims to identify and characterize the main challenges for GNSS measurements in urban environments, supporting which techniques provide a more reliable output within the variability of environmental constraints. The aims are to provide a quantitative comparison of positional errors for each method and practical recommendations to improve positioning accuracy in an urban environment; investigation of alternative or hybrid techniques, such as combining GNSS with total station surveys or GNSS-INS systems, will provide high precision positioning for applications involving autonomous navigation and urban geodesy.

Materials and Methods

CORS-VRS

A Virtual Reference Station (VRS) is a simulated GNSS reference point designed to enhance real-time positioning accuracy. By leveraging data from a network of continuously operating reference stations (CORS), VRS creates a localized correction signal, reducing spatial errors and improving RTK (Real-Time Kinematic) precision. This allows users to achieve centimeter-level accuracy as if a reference station were positioned at their exact location (Ghilani and Wolf, 2012).

PPK Survey

Post-Processing Kinematic is a GNSS data processing method used to achieve high-accuracy positioning by correcting errors in the raw positioning data. It is widely used in applications where precise geospatial information is critical, such as surveying, mapping, and UAV operations (Ghilani and Wolf, 2012).

Static Survey

GNSS surveying with the static method is widely used to calculate high-precision tri-dimensional coordinates in traverse stations: these systems provide coordinates of ground locations at a millimeter level both in the horizontal and vertical components (Ghilani and Wolf, 2012).

As explained above, the experiment was carried out in Esenler, Istanbul, Turkey (Figure 1). The site was selected in the medium-rise, Gencosman District, Esenler. The selection of the survey points was done in such a manner that P1, P2, and P3 could represent different kinds of urban GNSS positioning challenges, considering the aims of the study. P1 is in a narrow street lined with 4-5-story buildings on both sides and simulates a high-obstruction environment where severe signal blockage and multipath effects are expected, hence ideal for testing GNSS accuracy in dense urban areas. P2 represents transitional urban conditions, sited in a moderate-obstruction area with partial sky visibility. Its conditions, therefore, allow assessment of GNSS performance under intermittent blockages. P3 represents the open-sky control point to provide baseline

reference and can be used to compare directly with total station measurements to indicate the maximum achievable accuracy of GNSS in good conditions. From the discussion of these three aspects, this research systematically analyses the impact of urban infrastructure on GNSS methods, namely CORS-VRS, PPK, and statistics, which are very important for their applicability in urban surveying and positioning accuracy in different obstruction conditions.

The three points to be measured were fixed with either asphalt nails. All static GNSS surveys were performed using one Topcon Hiper HR receiver. Static GNSS surveys were performed to determine the coordinates of these three points. The surveys in this primary network were conducted with at least 2 hours of observation times. The minimum elevation cut-off angle and the sample rate were 10 degrees and 30 seconds, respectively. The performance specifications of the Topcon Hiper HR receivers are 8 mm+1.0 ppm for horizontal and 15 mm+1.0 ppm for vertical positioning (kinematic); 2.5 mm+1.0 ppm for horizontal and 5 mm+1.0 ppm for vertical positioning (static). For this study, P1 and P2 were in urban environments, but P3 was located in an unobstructed area (Figures 2 and 3).

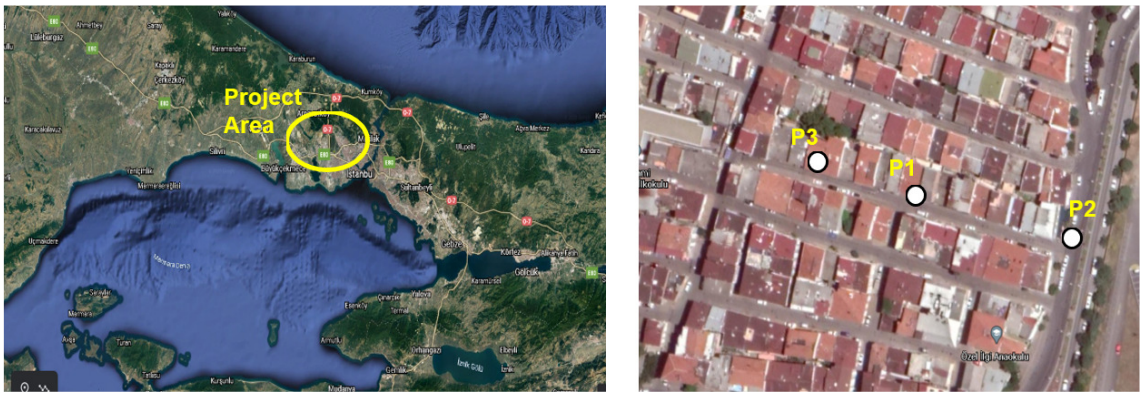

Figure 1. Project area and three points (P1, P2 and P3) in the project site

Figure 2. Station P1, P2 and P3 in the urban areas and the unobstructed area

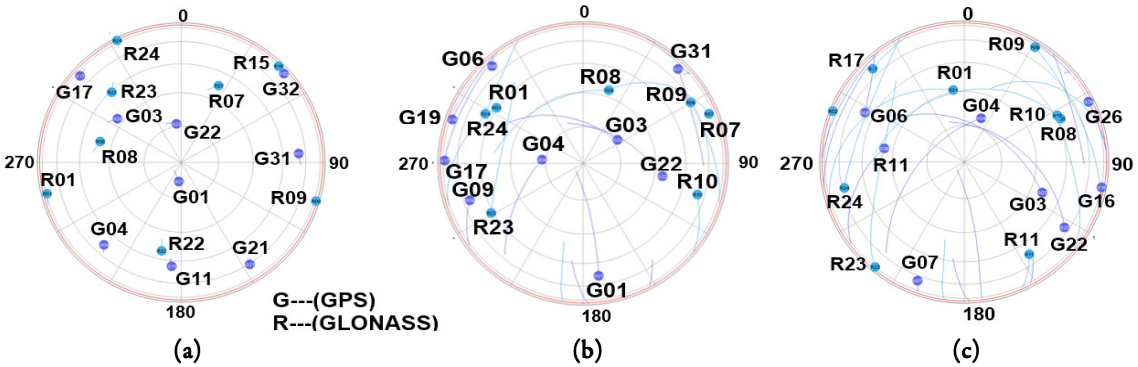

Figure 3. Skyplots at P1 **(a)**, and P2 **(b)**, strong obstruction by the buildings; skyplot at P3 **(c)** in the unobstructed area between 11:11:46 and 13:44: 30 hours on 30 September 2020

As known, the buildings caused severe obstruction of the sky for these two points (especially for P1 and P2 points) in the project area (Figures 1, 2 and 3). The problem shown by the sky plot of 11:11–13:44 hours is typical for the whole day: several satellites were shaded by the buildings but were still tracked by the receivers (Figures 3a and 3b). But all observed satellites for P3 point were not shaded due to the clear-line-of sight (Figure 3c).

Results

Static Processing

For reliable positioning, it has been stated that at least 30 minutes is needed, although better results are obtained with increasing time (Gao *et al.*, 2018). In static GNSS observation, two-hour measurement can provide sufficient data to reduce the effects of random errors and increase positioning reliability by providing sub-centimeter accuracy. Studies show that when the environment is more multipath and signal obstacle, the general trend of solutions from GNSS is better with increasing measurement time (Ge *et al.*, 2018; Wu *et al.*, 2019). Data processing and network adjustments were carried out using Topcon Magnet Tools Software. In the adjustment procedure, ITRF 2014 coordinates 2020.50 epoch of PALA point (ISKI-CORS point being used in Istanbul, 30 September 2020 weather forecast for Istanbul: Partly and partly cloudy) were held fixed (Table 1). The ISKI-CORS station PALA was about 10 km away from the project site. Table 2 illustrates the time schedule of the VRS measurements for three points (P1, P2, and P3) by using Topcon Hiper VR receivers.

Table 1. The Cartesian coordinates and their standard deviations of the three points in ITRF 2014 coordinate 2020.5 epochs (30 September 2020)

Name	X (m)	Y (m)	Z (m)	Std X (mm)	Std Y (mm)	Std Z (mm)
PALA	4212288.674	2331374.789	4169766.761	0	0	0
P1	4218722.976	2327940.148	4165119.730	4	4	9
P2	4218759.206	2328041.342	4165036.134	3	2	6
P3	4218742.050	2327978.624	4165084.650	2	5	11

Table 2. Time schedule of the VRS measurements for three points (P1, P2, and P3) by using Topcon Hiper VR receivers

Date Time	Point	X	Y	Z	Ep.	Hz	SAT.	hRms	vRms	Pdop	Method	Status
2020-09-30-12:44:30	P1	4218723,064	2327939,696	4165119,188	5	1	12	0,004	0,006	1,689	VRS	FIX
2020-09-30-13:44:30	P2	4218759,481	2328041,078	4165036,100	5	1	14	0.002	0.004	1.345	VRS	FIX
2020-09-30-11:11:46	P3	4218741,898	2327977,991	4165084,297	5	1	7	0,013	0,017	4,482	VRS	FIX

Post-Process Kinematic (PPK) Method

Although kinematic data collection has the advantage of high productivity, it has some disadvantages. Accuracy is not as well as with static data collection. The impact of the bad signal quality on the positioning results is naturally worse for kinematic positioning than for static processing occurs. Kinematic surveying can provide immediate results using the real-time kinematic mode or in the office using the post-process kinematic mode (Pirti 2016).

In this study, the static GNSS survey results for P1, P2 and P3 points were compared with PPK survey results. The PPK (epoch-by-epoch) derived coordinates of the three points (P1, P2 and P3) were compared with their coordinates as precisely determined by using static surveys. The static survey was performed to control and evaluate the performance of the PPK surveys. Figure 4 shows the results of epoch-by-epoch kinematic processing (PPK) of about 2 hours session for the P1, P2 and P3 points by using kinematic CSRS-PPP solution from dual frequency GPS + GLONASS observations and final precise ephemeris at 95% confidence level.

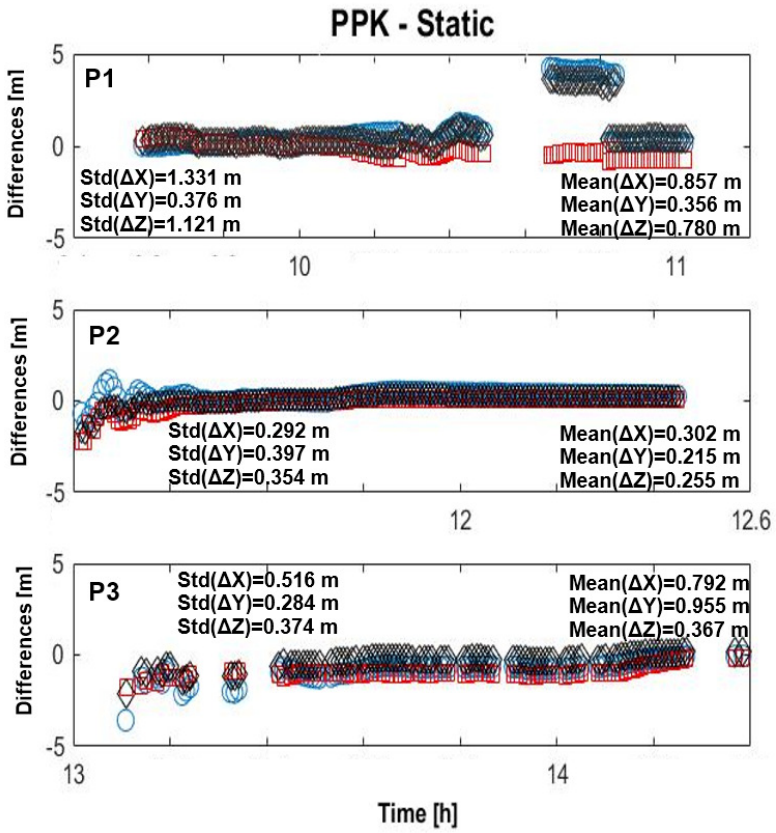

Figure 4. Epoch-by-epoch horizontal coordinate results of P1, P2 and P3 points by using post-processed kinematic module, deviation from static results

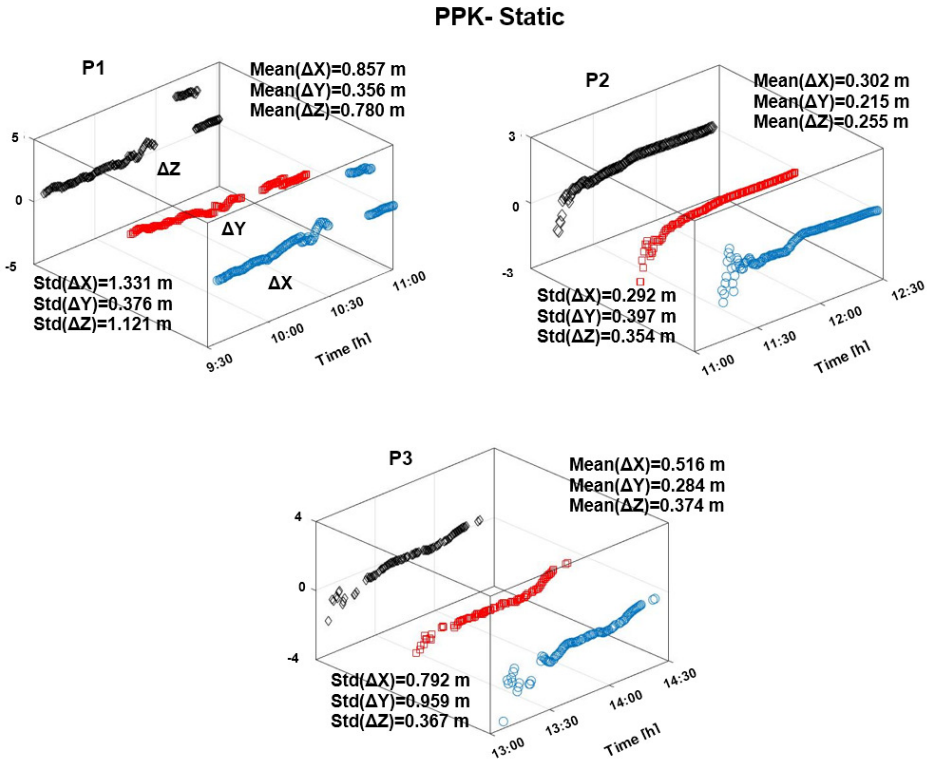

Figure 5. Epoch-by-epoch the three-dimensional coordinate results of P1, P2 and P3 points by using post-processed kinematic module, deviation from static results on 30 September 2020

Figures 4 and 5 shows standard deviations and mean values of P1, P2 and P3 points, in X, Y, Z coordinate components. The largest variations in the coordinates were recorded for the two points (P1, P3) in the study area. The comparison of the results of the PPK and static surveys for P1 point shows that the variations were generally about ± (1-420) cm in horizontal and vertical coordinates between 9:30:00 hour and 11:00:00 hour (except for between 10:30-10:40 hour) (Figure 4). The ambiguity solution is not fixed at this period. Signal scattering due to the buildings causes strongly fluctuating epoch results for the X, Y and Z components (Figure 4). The minimum difference of the X coordinates for P1 point is about 1 cm; the minimum difference of the Y coordinates is about 6 cm, and the minimum difference of the Z coordinates is about 20 cm at the same epoch of the survey time. The standard deviation values of X, ΔY and ΔZ are 1.331 m, 0.376 m and 1.121 m respectively. The mean values of the ΔX, ΔY and ΔZ are 0.857 m, 0.356 m and 0.780 m respectively. The comparison of the results of the PPK and static surveys for P2 point shows that the variations were generally about ± (1-225) cm in horizontal and vertical coordinates between 9:30:00 hour and 11:00:00 hour (Figure 4). Scattering due to the buildings and vehicles causes strongly fluctuating epoch results for the X, Y and Z components (Figure 4). The minimum difference of the X coordinates for P2 point is about 0.1 cm; the minimum differences of the Y coordinates is about 2.2 cm, and the minimum differences of the Z coordinates are about 10 cm at the same epoch of the survey time. The standard deviation values of X, ΔY and ΔZ are 0.292 m, 0.397 m and 0.354 m respectively. The mean values of the ΔX, ΔY and ΔZ are 0.302 m, 0.215 m and 0.255 m respectively. The comparison of the results of the PPK and static surveys for P3 points shows that the variations were generally about ± (1-300) cm in horizontal and vertical coordinates between 13:00 and 14:30 hour (Figures 4 and 5). The ambiguity solution is not fixed at some periods. Signal scattering due to the buildings causes strongly fluctuating epoch results for the X, Y and Z components (Figure 4). The minimum difference of the X coordinates for P1 point is about 6.4 cm; the minimum difference of the Y coordinates is

about 14.2 cm, and the minimum difference of the Z coordinates is about 15 cm at the same epoch. The standard deviation values of the ΔX, ΔY and ΔZ are 0.792 m, 0.959 m and 0.367 m respectively. The mean values of the ΔX, ΔY and ΔZ are 0.516 m, 0.284 m and 0.374 m respectively.

It is clear that all of the results show that buildings were harmful to PPK positioning, as they frequently blocked the signals of the low-medium-high satellites and affect radio signals. This phenomenon is justified as it was seen in all tests at the same locations. Thus, even with the presence of good satellite windows, signal blockage due to buildings could be considered as the main problem affecting the use of PPK in urban areas. The X and Y coordinate differences between PPK and static surveys obtained at these two points (P1 and P3) in the urban area remained in the range of 6-15 cm in only one epoch in this study. The differences of Z coordinates were obtained in the range of 15-20 cm for P1 and P3 points in the epochs of the survey time. As a result of the processing for P1, the X and Y coordinate differences between kinematic (155 epochs) and static remained in the range of about 1 cm to 6 cm in only one epoch. As for P3, the X and Y coordinate differences between kinematic (97 epochs) and static remained in the range of about 6 cm to 15 cm in only one epoch. The Z coordinate differences for P1 and P3 between kinematic and static remained in the range of about 15-20 cm in the same epoch mentioned above. As for P2, the multipath effect differs from the other two points. P2 is located approximately outside the urban areas and is 12 meters away from the urban areas. Although P2 was not affected by the multipath effect as much as P1 and P3 points. It was still exposed to this multipath effect in a small amount (Figure 5).

Figure 6 shows the differences and their means and standard deviation values for the three points. All of the results show that buildings were harmful to CORS-VRS positioning, as they frequently blocked the signals of the low-medium-high satellites and affect radio signals. The phenomenon is validated by its consistent observation in every test conducted at the same locations. Thus, even with the presence of good satellite windows, signal blockage due to buildings could be considered as the main problem affecting use of CORS-VRS in urban areas. The ambiguity resolution time was approximately 60-90 minutes for the two points (P1 and P2) in the urban areas.

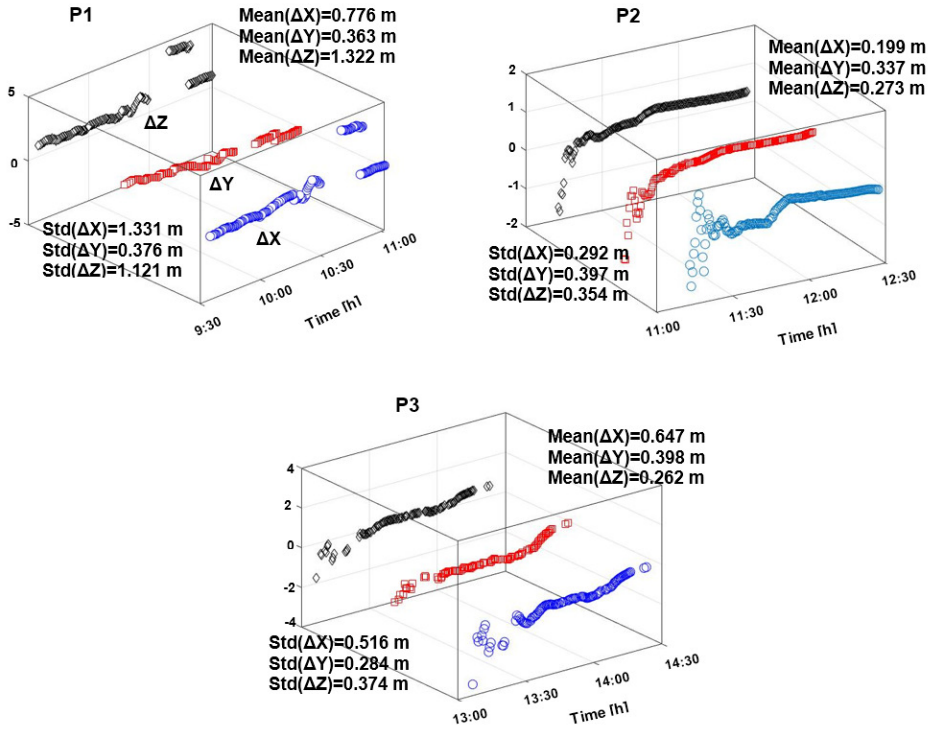

Figure 6. Epoch-by-epoch the three-dimensional Cartesian coordinate results of P1, P2 and P3 points by using post-processed kinematic (PPK) module, deviation from CORS-VRS results

The static method provides a significant advantage due to the ability to use all data over a long period of time in urban environments where satellite visibility is constantly changing. In contrast, PPK relies on real-time data processing, which can be adversely affected by temporary signal interruptions or reflections, which reduce reliability. Since static GNSS observations collect data over a longer period, they help eliminate the effects of multipath and signal degradation, which increases accuracy (Zhang and Hsu, 2018; Yuan *et al.*, 2022). Therefore, static methods perform better than PPK in such challenging environments.

Total Station Surveys and Comparisons

The quality of the GNSS results can be assessed by comparison with the slope distances determined by the terrestrial measurements. To compare the results of CORS-VRS, static with those of independent measurement method, the slope distances were surveyed among the three points (P1, P2 and P3) by using a total station (Figure 7). The slope distances were recorded with Topcon OS-103 (angle accuracy: ± 3", distance measurement accuracy: 2 mm + 2ppm). Table 3 shows the slope distance differences of the three points between static and total station surveys.

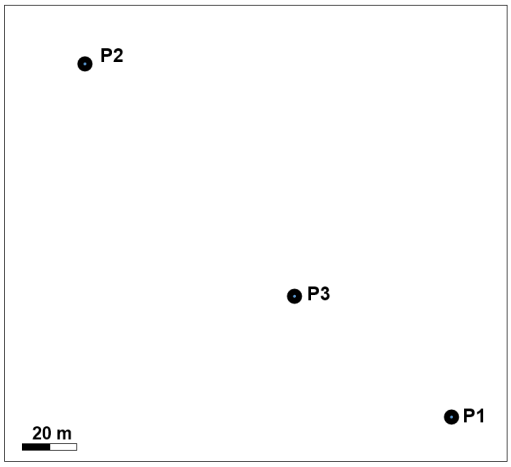

Figure 7. The distribution of the three points in the project area

Table 3. Comparison of the slope distances among the three points in the project area between total station and static GNSS surveys

Baseline	Static GNSS	Total Station	Differences (m)
	Slope Distance [S] (m)	Slope Distance [S] (m)	
P1-P2	136.166	136.175	−0.009
P2-P3	81.139	81.139	−0.006
P1-P3	55.445	55.459	−0.014

Table 3 illustrates comparison of the slope distances results between the static GNSS, and total station surveys show that the variations were 0.6-1.4 cm in slope distances. The maximum differences of the slope distances are about 1.4 cm for P1-P3 baselines in this study because these two points (P1 and P3) are located in the urban environments.

Table 4 shows the slope distance differences among the three points between CORS-VRS and total station surveys. The comparison of the results of the CORS-VRS and total station surveys shows that the variations were about 13-34 cm among slope distances. The maximum differences among the three slope distances are about 34 cm for P1-P3 baselines in this study because these two points (P1 and P3) are in the urban environments.

Table 4. Comparison of the slope distances among the three points in the project area between total station and CORS-VRS surveys

Baseline	CORS-VRS	Total Station	Differences (m)
	Slope Distance [S] (m)	Slope Distance [S] (m)	
P1-P2	136.045	136.175	−0.130
P2-P3	81.315	81.139	−0.176
P1-P3	55.124	55.459	−0.335

With the increasing number of satellites increase the satellite will increase the satellite availability and improve the geometry but positioning in urban areas, these problems persist for CORS-VRS and PPK methods.

Consistency among the VRS, Static, and PPK Results

To check the compatibility of the PPK technique with the static technique, the three-dimensional (3D) misclosure vectors were computed as follows (Pirti 2013):

$$m_P^2 = (X_{PPK} - X_{Static})^2 + (Y_{PPK} - Y_{Static})^2 + (Z_{PPK} - Z_{Static})^2 \quad (1)$$

where m_P is the misclosure vector (in meters) for all of the points, Y_{PPK} and X_{PPK} are the Cartesian coordinates (in meters) of the three points from PPK survey coordinates, Y_{Static} and X_{Static} are the Cartesian coordinates of the three points (P1, P2 and P3) from static surveys.

Figures 8 and 9 show the horizontal misclose vectors for these three points. In this study the most important criteria in PPK measurement technique are survey time and fixed of the integer ambiguity values. Except for the partial and float ambiguity solutions for P1, P2 and P3 points within urban and unobstructed environments (Figure 8), the results clearly show that the PPK technique is a stable method and about ± (5-20) cm level of accuracy is generally obtainable (Figure 8b) for three points. Figure 9 shows the obtained differences among three points show that the CORS-VRS technique is not a stable method in the urban areas and about ±(50-100) cm level of accuracy is generally obtainable (Figure 9b) for the three points.

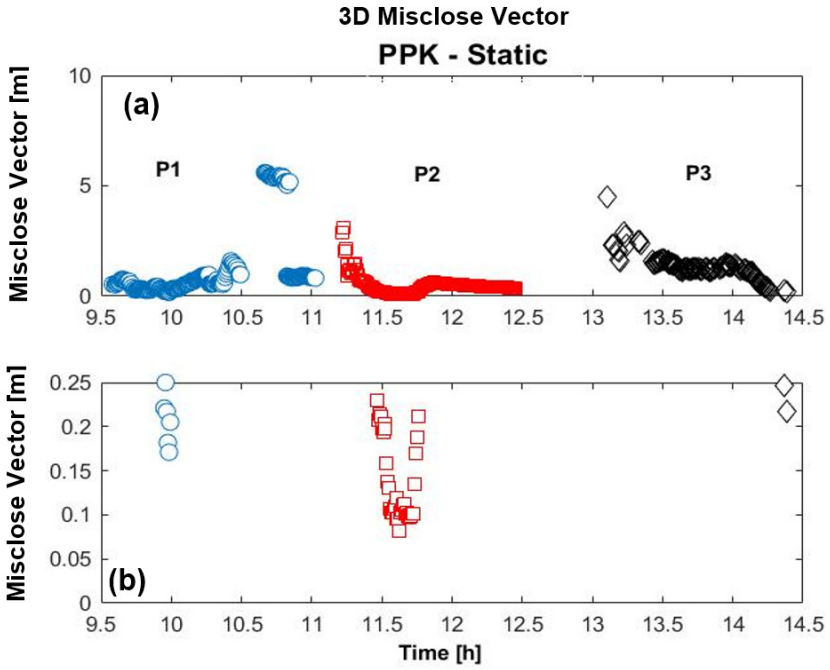

Figure 8. (a) 3D misclosure vectors for all three points (between PPK and static) in the project area and **(b)** below 0.25 m

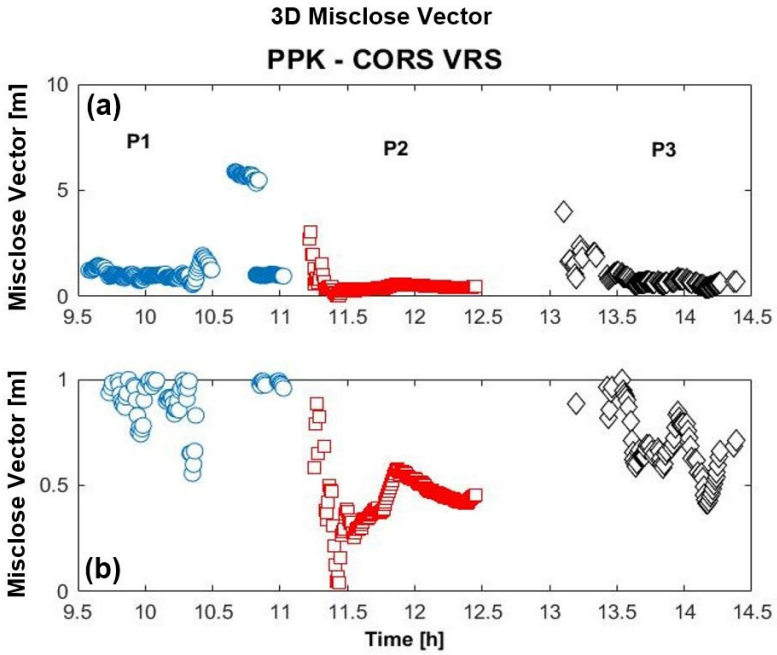

Figure 9. (a) 3D misclosure vectors for all three points (between PPK and static) in the project area and **(b)** below 1 m

In this study, it was demonstrated that Cartesian coordinates must be used to achieve tolerable errors in engineering applications. In addition, since there is a direct relation between better accuracy, precision and larger occupation time, and the hour of the day had no relevant effect, it is better to consider the multipath effect to guarantee the quality of control points with static GNSS positioning. An alternative method of performing a kinematic survey is to collect the data and process it at a later time. This does not require the use of a communications link (i.e. radio or cell phone) and can be combined with CORS-VRS to perform infill when the link is temporarily down. Post-processed kinematic survey methods provide the surveyor with a technique for high production surveys and can be used in areas with minimal obstructions of the satellites. PPK uses significantly reduced observation times (i.e. 0.5 to 3 minutes, usually 10-30 seconds per point) compared to static observations. This method requires a least squares adjustment or other multiple baseline statistical analysis capable of producing a weighted mean average of the observations. Post-processing will allow kinematic surveying to be used for some Level 3 surveys (Total baseline length error at 2σ, 12 mm + 1 ppm; Horizontal accuracy at 2σ, 25 mm). However, the accuracy of the PPK results remained in the range of 10-25 cm.

Discussion

This study highlights the significant impact of urban environments on GNSS positioning accuracy, particularly when using CORS-VRS and PPK methods. The comparative analysis of static GNSS, PPK, and CORS-VRS measurements against total station data demonstrated that static GNSS positioning provided the most precise results, with horizontal errors below 5 mm and vertical errors below 11 mm, making it the most reliable method in urban conditions. In contrast, PPK measurements exhibited mean deviations ranging from 0.215 m to 0.857 m across different test points, showing increased sensitivity to multipath effects and signal blockages. The most affected method was CORS-VRS, with baseline distance errors between 13 cm and 34 cm, demonstrating that real-time kinematic (RTK)-based solutions are highly vulnerable to urban obstructions.

The performance of GNSS positioning varied significantly across the three test points due to differing levels of obstruction. P1, located in a dense urban area, experienced the highest positioning errors due to severe satellite signal blockages and strong multipath interference. P2, situated in a moderately obstructed area, showed relatively better accuracy but was still affected by occasional signal degradation. P3, placed in an open-sky environment, served as a control point, confirming that GNSS positioning can achieve high accuracy when obstruction-free conditions are met. These findings indicate that GNSS methods relying on real-time corrections, such as CORS-VRS, may not always provide consistent accuracy in urban environments, necessitating the integration of alternative positioning methods like total stations or hybrid GNSS-Inertial Navigation Systems (INS).

Furthermore, multipath effects remain a critical challenge in urban positioning. To eliminate/minimize the multipath effect, care should be taken to ensure that there are no reflective surfaces around the location where the GNSS receiver is installed. In addition, various equipment and techniques, such as choke ring antennas, low multipath antennas, and high gain antennas, can be used to minimize multipath effects in applications. This effect can be eliminated by taking measures such as GNSS receivers equipped with signal processing algorithms, signal-to-noise ratio (SNR) filters, wavelet transform filtering, and a Mischke filter that reduces errors in carrier phase measurements (Tamazin *et al.*, 2016; Sun *et al.*, 2018). The fluctuating results in PPK and CORS-VRS measurements highlight the need for advanced signal processing techniques, such as machine learning-based multipath mitigation (Li *et al.*, 2020) or integrating multi-constellation GNSS to increase satellite availability (Wen *et al.*, 2018; Zhang *et al.*, 2022; Hamza *et al.*, 2023). Future studies should focus on improving positioning algorithms, particularly for real-time applications in urban areas, where maintaining centimeter-level accuracy is essential for applications such as autonomous navigation and urban geodetic surveys (Viler *et al.*, 2023).

In conclusion, while static GNSS remains the most reliable approach for urban surveys, CORS-VRS and PPK techniques can still be valuable for applications where moderate accuracy (10-25 cm) is acceptable. However, their performance is highly dependent on satellite visibility and environmental conditions. The results of this study emphasize the importance of selecting appropriate survey techniques based on environmental constraints and highlight the potential for future improvements through advanced error correction and hybrid positioning solutions.

Conclusions

GNSS is used in urban environments that is particularly challenging to the GNSS signal reception due to multipath and direct signal blockages, which significantly affect the signal processing and further degrade the position accuracy and availability. In this study the most important criteria in PPK, CORS-VRS measurement technique are survey time and fixed of the integer ambiguity value. Nonetheless, it appears that urban measurements with ± 1 cm accuracy cannot be guaranteed on all occasions, since urban areas may lead to greater errors (10-25 cm). GPS and GLONASS observations in processing static sessions conducted under conditions of limited satellite availability give better results in this study.

To overcome this problem, the inclusion of GNSS systems such as Beidou and Galileo in the measurements increases the number of observed satellites and thus can contribute positively to the obtained results. In future studies, it is aimed to statistically examine the effects of these GNSS systems on positioning accuracy.

Authors' Contributions

Both authors contributed to the manuscript at all stages of the work (conceptualization, data curation, formal analysis, funding acquisition, investigation, methodology, project administration, resources, software, validation, visualization, writing). Both authors read and approved the final manuscript.

Acknowledgments

This research received no specific grant from any funding agency in the public, commercial, or not-for-profit sectors.

Conflict of Interests

The authors declare that there are no conflicts of interest related to this article.

References

Chen S, Liu H, Feng Z, Shen C, Chen P (2019). Applicability of personal laser scanning in forestry inventory. PLoS ONE 14(2):e0211392. *https://doi.org/10.1371/journal.pone.0211392*

El-Mowafy A (2000). Performance analysis of the RTK technique in an urban environment. Australian Surveyor 45(1):47-54. *https://doi.org/10.1080/00050353.2000.10558803*

Erenoglu RC, Erenoglu O, Arslan N (2018). Accuracy assessment of low cost UAV based city modelling for urban planning. Tehnički Vjesnik 25(6):1708-1714. *https://doi.org/10.17559/TV-20170904202055*

Feng X, Zhang T, Lin T, Tang H, Niu X (2020). Implementation and performance of a deeply-coupled GNSS Receiver with low-cost MEMS inertial sensors for Vehicle Urban Navigation. Sensors 20(12):3397. *https://doi.org/10.3390/s20123397*

França RMD, Klein I, Veiga LAK (2021). The influence of the deflection of the vertical on geodetic surveys in Brazil. Boletim de Ciências Geodésicas 27(spe):e2021020. *https://doi.org/10.1590/s1982-21702021000s00020*

Gallo KP (2002). Satellite-based detection of global urban heat-island temperature influence. Journal of Geophysical Research 107(D24):4776. *https://doi.org/10.1029/2002jd002588*

Gao F, Xu T, Wang N, Jiang C, Du Y, Nie W, Xu G (2018). Spatiotemporal evaluation of GNSS-R based on future fully operational global multi-GNSS and eight-LEO constellations. Remote Sensing 10(2):67. *https://doi.org/10.3390/rs10010067*

Ge H, Li B, Ge M, Zang N, Nie L, Shen Y, Schuh H (2018). Initial assessment of precise point positioning with LEO enhanced Global Navigation Satellite Systems (LeGNSS). Remote Sensing 10(7):984. *https://doi.org/10.3390/rs10070984*

Ghilani CD, Wolf PR (2012). Elementary surveying: An introduction to geomatics (13th ed). Prentice Hall.

Hamza V, Stopar B, Sterle O, Pavlovčič-Prešeren P (2023). Low-cost dual-frequency GNSS receivers and antennas for surveying in urban areas. Sensors 23(5):2861. *https://doi.org/10.3390/s23052861*

Hayamizu M, Nakata Y (2023). Accuracy assessment of post-processing kinematic georeferencing based on real-time kinematic unmanned aerial vehicles and structure-from-motion photogrammetry: Topographic measurements of a riverbed in a small watershed with a check dam. Authorea Preprints.

James MR, Quinton JN (2013). Ultra-rapid topographic surveying for complex environments: the hand-held mobile laser scanner (HMLS). Earth Surface Processes and Landforms 39(1):138-142. *https://doi.org/10.1002/esp.3489*

Jones N, Manconi A, Löw S (2022). Satellitenfernerkundung der räumlichen und zeitlichen Entwicklung der Oberflächendeformationen [Satellite remote sensing of the spatial and temporal development of surface deformations]. Schweizerische Zeitschrift für Forstwesen 173(3):118-123. *https://doi.org/10.3188/szf.2022.0118*

Li Q, Xia L, Chan TO, Xia J, Geng J, Zhu, H, Cai Y (2020). Intrinsic identification and mitigation of multipath for enhanced GNSS positioning. Sensors 21(1):188. *https://doi.org/10.3390/s21010188*

Li X, Wang H, Li S, Feng S, Wang X, Liao J (2021). GIL: A tightly coupled GNSS PPP/INS/LiDAR method for precise vehicle navigation. Satellite Navigation 2:26. *https://doi.org/10.1186/s43020-021-00056-w*

Mai NTT, Chi NTM, Hung ND, Khanh DN (2022). Analyze development potential in affected areas adjacent to urban public transit systems. Case study in the stations of Kim Ma and Van Phuc 2 (BRT Line No. 1). Journal of Science and Technology in Civil Engineering (JSTCE)-HUCE 16(4):58-72. *https://doi.org/10.31814/stce.nuce2022-16(4)-05*

Ning Y, Wang J, Han H, Tan X, Liu T (2018). An optimal radial basis function neural network enhanced adaptive robust Kalman filter for GNSS/INS integrated systems in complex urban areas. Sensors 18(9):3091. *https://doi.org/10.3390/s18093091*

Pirti A (2016). The seasonal effects of deciduous tree foliage in CORS-GNSS measurements (VRS/FKP). Tehnički Vjesnik 23(3):769-774. *https://doi.org/10.17559/TV-20150301214046*

Pirti A, Yücel M, Gumus K (2013). Testing real-time kinematic GNSS (GPS and GPS/GLONASS) methods in obstructed and unobstructed sites. Geodetski Vestnik 57(3):498-512.

Sideris M (2014). Geodetic world height system unification. In: Freeden W, Nashed M, Sonar T (Eds). Handbook of Geomathematics. Springer, Berlin, Heidelberg. *https://doi.org/10.1007/978-3-642-27793-1_83-1*

Sun C, Zhao H, Feng W, Du C. (2018). A frequency-domain multipath parameter estimation and mitigation method for BOC-modulated GNSS signals. Sensors 18(3):721. *https://doi.org/10.3390/s18030721*

Suzuki T, Kubo N (2015). Simulation of GNSS satellite availability in urban environments using Google Earth. Proceedings of the ION 2015 Pacific PNT Meeting, Honolulu, Hawaii, April 2015, pp 1069-1079.

Tamazin M, Noureldin A, Korenberg MJ, Kamel AM (2016). A new high-resolution GPS multipath mitigation technique using fast orthogonal search. Journal of Navigation 69(4):794-814. *https://doi.org/10.1017/s0373463315001022*

Viler F, Cefalo R, Sluga T, Snider P, Pavlovčič-Prešeren P (2023). The efficiency of geodetic and low-cost GNSS devices in urban kinematic terrestrial positioning in terms of the trajectory generated by MMS. Remote Sensing 15(4):957. *https://doi.org/10.3390/rs15040957*

Wang J (2023). Sky-view images aided NLOS detection and suppression for tightly coupled GNSS/INS system in urban canyon areas. Measurement Science and Technology 35(2):025112. *https://doi.org/10.1088/1361-6501/ad087f*

Wang M, Yan X (2015). A comparison of two methods on the climatic effects of urbanization in the Beijing-Tianjin-Hebei metropolitan area. Advances in Meteorology 2015:52360. *https://doi.org/10.1155/2015/352360*

Wang Y, Liu P, Liu Q, Adeel M, Qian J, Jin X, Ying R (2019). Urban environment recognition based on the GNSS signal characteristics. Navigation 66(1):211-225. *https://doi.org/10.1002/navi.280*

Wen W, Zhang G, Hsu LT (2018). Exclusion of GNSS NLOS receptions caused by dynamic objects in heavy traffic urban scenarios using real-time 3D point cloud: An approach without 3D maps. 2018 IEEE/ION Position, Location and Navigation Symposium (PLANS), pp 158-165. *https://doi.org/10.1109/plans.2018.8373377*

Wu Q, Sun M, Zhou C, Zhang P (2019). Precise point positioning using dual-frequency GNSS observations on smartphone. Sensors 19(9):2189. *https://doi.org/10.3390/s19092189.*

Xie P, Petovello MG (2014). Measuring GNSS multipath distributions in urban canyon environments. IEEE Transactions on Instrumentation and Measurement 64(2):366-377. *https://doi.org/10.1109/TIM.2014.2342452*

Yang X, Ruby Leung L, Zhao N, Zhao C, Qian Y, Hu K, ... Chen B (2017). Contribution of urbanization to the increase of extreme heat events in an urban agglomeration in East China. Geophysical Research Letters 44(13):6940-6950. *https://doi.org/10.1002/2017gl074084*

Yuan R, Xie S, Li Z, He Z (2022). Adaptive fast independent component analysis methods for mitigating multipath effects in GNSS deformation monitoring. Journal of Sensors 2022(1):4604950. *https://doi.org/10.1155/2022/4604950*

Zhang G, Hsu LT (2018). Intelligent GNSS/INS integrated navigation system for a commercial UAV flight control system. Aerospace Science and Technology 80:368-380. *https://doi.org/10.1016/j.ast.2018.07.026*

Zhang G, Xu P, Xu H, Hsu LT (2021). Prediction on the urban GNSS measurement uncertainty based on deep learning networks with long short-term memory. IEEE Sensors Journal 21(18):20563-20577. *https://doi.org/10.1109/JSEN.2021.3098006*

Zhang J, Khodabandeh A, Khoshelham K (2022). Centimeter-level positioning by instantaneous LiDAR-aided GNSS ambiguity resolution. Measurement Science and Technology 33(11):115020. *https://doi.org/10.1088/1361-6501/ac82dd*

Zhou L, Dickinson R, Tian Y, Fang J, Li Q, Kaufmann R, Myneni R (2004). Evidence for a significant urbanization effect on climate in China. Proceedings of the National Academy of Sciences 101(26):9540-9544. *https://doi.org/10.1073/pnas.0400357101*